

Design and Analysis of the Independent Communication Module for LESPA- Lunar Electric Surface Potential Analyzer

Arunima Prakash^{1*}, Diwakar R. Marur², Sakshi Namdeo³

¹Student, Department of ECE, SRM Institute of Science and Technology

²Associate Professor, Department of ECE, SRM Institute of Science and Technology

³Student, Department of ECE, SRM Institute of Science and Technology

*Corresponding author E-mail: arunimaprakash_omitabhsaran@srmuniv.edu.in

Abstract

Moon, our closest celestial neighbor and Earth's only natural satellite is of utmost scientific importance. So far there have been 67 missions to the Moon, thus to enhance and aid further research understanding of lunar surface is vital. The Moon meets the Earth's magnetotail (an extension of Earth's magnetosphere) twice in a month encountering a gigantic sheet of ionized particles or plasma. These charged particles intersperse on the lunar dust and give it a negative charge. The electric field created by this phenomenon creates a substantial potential difference across the two sides of the lunar surface. Electrified dust grains can adhere to machinery and the large electric fields can affect electronics of landers or payload machinery. A payload is proposed Lunar Electric Surface Potential Analyzer (LESPEA) to measure the effects of these magnetotail crossings. LESPEA will need to establish a low BER link with the in-orbit lunar satellite at optimum frequencies to relay the raw data. This paper aims to analyze and study the link budget requirements for designing an Independent Communication Module (ICM) for LESPEA as well as antenna models for the transmitter. The scope of the designed ICM is to ultimately assist in designing lander missions for future lunar exploration and aid in future lunar exploration missions and colonization activities.

Keywords: antenna modelling; LESPEA; link budget; Lunar communication; visibility analysis.

1. Introduction

The Moon, our nearest celestial neighbor, is of crucial scientific importance and is the base target for space exploration because it represents a body frozen in time that in itself, has records of some of the earliest processes in solar system evolution (e.g., planetary differentiation, impact flux, and processes). The oldest material excavated from the surface of the Moon by the lunar missions is estimated to be around the same age as that of the solar system; 5 billion years. The Moon represents a celestial body preserving the unique history of planetary formation, space environment, and cosmic radiations for years, which has not been erased by weathering or any other evolutionary processes as in the case of the Earth. There is no atmosphere on Moon and a subsurface abundance of igneous (fire formed) rocks. Seeing through the early history of chemical segregation, bombardment and volcanism to the Moon's primordial origins is one of the prime objectives of space science [1].

The stratigraphy of the Moon comprises of the top 'rolling' layer of powdery soil and fragments of moon rocks called the 'Regolith.' The source of regolith formation is linked to the meteoritic impacts which formed the craters [2].

1.1. Lunar Dust

Dust is an easy fraction of the Lunar regolith that is less than 20 μm in diameter and it makes up some of 10 to 15% of the soil. Apollo 17 soil samples contained up to 28% lunar dust. During the Apollo missions, we learnt that lunar dust was a serious problem.

It clings electrostatically to the surfaces and was difficult to remove and almost impossible in some cases. The dust would cling to the astronauts' helmet visor, obscuring vision. Attempts to wipe the dust off the visors resulted in scratches that also obscured vision. The dark dust grains absorb sunlight, thus the equipment covered in the lunar dust became excessively hot in some mission scenarios. This also resulted in a steady increase in temperature causing false readings in the instruments. The lunar Rovers had less traction than that was expected, and this was attributed to the fine lunar dust. The dust also affected the screens on the spacesuits and implicating the suits to lose their ability to maintain pressure within safe limits. For longer lunar missions, lunar soil is a severe safety issue. The severity of the dust problem was constantly consistently underestimated by ground tests indicating a need to develop a better simulation facilities and procedures.

1.2. Lunar Magnetotail Crossing

The lunar environment causes the dust to have some surprising qualities. The lunar regular it is completely devoid of moisture at all the sites that have been sampled by the Apollo and Luna missions. Since the Moon lacks an atmosphere galactic cosmic rays, solar ultraviolet radiation and solar wind particles reach the surface and interact with the regolith. Earth's magnetotail is a major cause for the abnormalities in the lunar dust. The Earth's magnetotail extends beyond the orbit of the moon. A magnetosphere is the region of space surrounding an astronomical object in which charged particles are controlled by that object's magnetic field. Planets with a magnetosphere, like Earth, are capable of mitigating or blocking the effects of cosmic radiation. This magnetosphere also has other effects on the objects orbiting the planet.

One such effect is the effect of Earth's magnetotail on the moon. The moon enters the magnetotail three days before it is full and takes about six days to cross and exit on the other side. During this crossing, the moon meets a gigantic sheet of ionized particles (Plasma). The lightest of these particles, the electrons pepper on surface of the moon and give it a negative charge. The photons incident on the bright side knock off the electrons on that side and keep the charge build up at relatively low levels. On the dark side, moon dust could get repelled by the negative charge and float and the difference in charge levels creates a potential difference between the two sides of the moon. As the Terminator line (the line between the day and the nightside) moves across the lunar surface dust is levitated and transported to higher altitudes. The dust could "flow" along this potential and could cause a dust storm. The electric field on the Lunar surface due to the magnetotail crossing can damage the on-board electronics of a lander. The Apollo surface experiment, the Lunar Ejector and Meteoroids Experiment (LEAM) detected an order-of-magnitude increase in the particles striking the detectors during local sunrise and sunset. During some crossings, the spacecraft sensed massive changes in the lunar night side voltage, jumping typically from -200 V to -5000V [3].

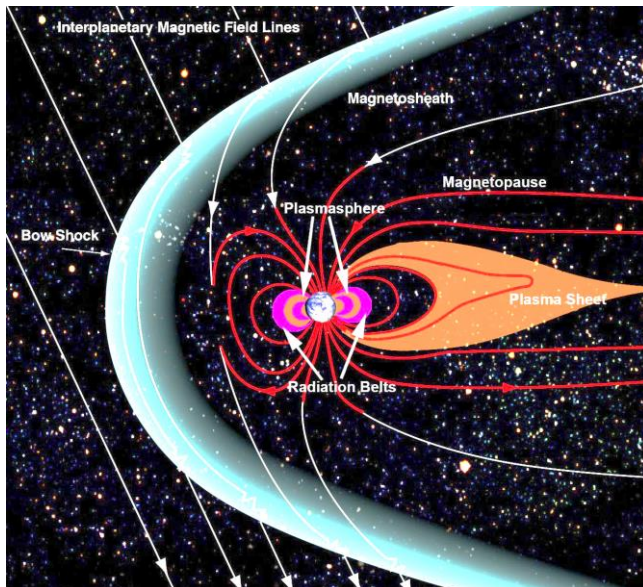


Fig. 1: Earth's Magnetotail[4]

1.3. LESPA

The Lunar Electric Surface Potential Analyzer (LESPA) is a spacecraft payload instrument for measuring the effects of these magnetotail crossings. This instrument aims to measure the electric field uses the principle of Electric Field Mill and it has been constructed in house for this study. LESPA can be tested, calibrated and regressively modelled for accurate measurements. It relays information to the on-orbit lunar satellite at optimum frequencies adhering to the link budget requirements. LESPA can be rebuilt with space grade components and standards and flown as a spacecraft payload for future lunar lander missions. Thus, the need to design an Independent Communication Module or ICM came to fulfil the communication needs of the LESPA, extending its role further to other viable payload options requiring a need to communicate back to the in-orbit satellite.

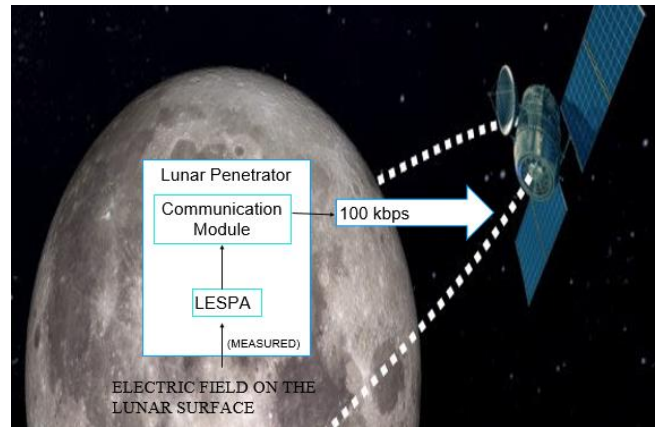


Fig. 2: System Architecture

1.4. Lunar Penetrator

The MIT Capstone-1 project configured the Lunar Surface Penetrator [2], housing as means to support small scale lunar missions. The Penetrator offers an array of assemblies such as a Global Positioning System (GPS) antenna for location information, solar power panels to generate electricity, disk braking to avoid over-penetration upon deployment, a sleek aluminum structure for rigidity and compartments for the ICM.

LESPA can be integrated with the various subsystems to sense, store, process and transmit data from the seismometers, GPS and overall wellness data. A tilt sensor, GPS antenna with card, and seismometer connect to an integrated computer board, which contains a flash memory unit, and both collects and stores the data obtained from the listed sensors. The integrated computer board will connect to the ICM computer that relays the data to an antenna, that connects to the orbiting satellite and acts as both a transmitter of information, as well as a receiver of commands. Power for all subsystem requirements is met through an available array of battery stacks - primary and secondary. The physical structure represents a nose cone, fitted at the front, which penetrates into the lunar ice and holds the housing in place, which also senses seismic data. The nose cone extends to a 0.8-meter-long cylinder that connects to external braking flare encircled on the exterior by a braking disc. This protects the primary battery pack, while the secondary is embodied in the after-body cylinder above the flare [2]. LESPA is designed such that it can be integrated on the Capstone Lunar Penetrator.

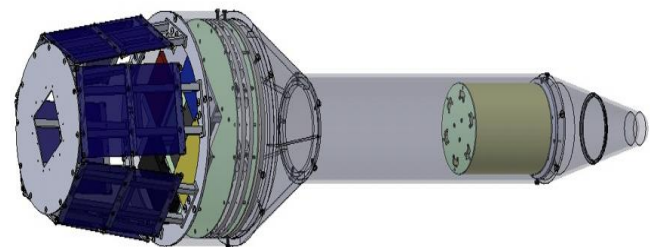


Fig. 3: 3D CAD model of the penetrator [2].

2. Independent Communication Model

The proposed methodology aims to model a completely independent and integrable communication module for assisting lunar exploration missions onboard the lunar penetrator. The Independent Communication Module (ICM) is designed as to support low to medium powered lunar payloads with minimal data rate requirements. The paper expands on the scope of designing a payload with 1W of peak transmitting power relaying the observed raw

data to the in-orbit lunar satellite orbiting in a 100km frozen which is simulated using Systems Tool Kit (STK) software. Further relay of data to the ground station on Earth is out of the scope of our research and is under the jurisdiction and control of external space agencies through their Deep Space Network (DSN) antennas. It is assumed that the satellite is visible within in look angles of the ICM. The satellite is carefully launched to perpetuate in a intersecting elevation, argument of perigee and the Right Ascension of Ascending Node (RAAN).

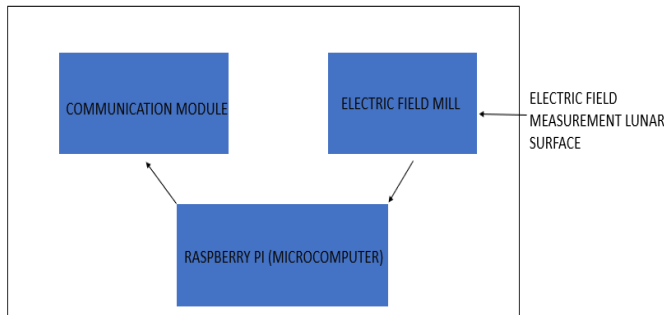


Fig. 4: Exploded view of the system architecture

2.1. Link Budget Analysis

As part of the modelling and analysis of the ICM module, a link budget was carried out to determine the optimum link requirements and specifications for establishing the communication link. Efficiency and performance of the link is dictated by the E_b/N_0 (Energy per bit by noise spectral density) and the BER performance. Hence, a dedicated link budget was formulated for a 100 kbps link, and BER of 10^{-6} using QAM and Reed Solomon coding to obtain actual realization of data [5].

$$E_b/N_0 = P + L_t + G_t + L_{pt} + L_{pr} + L_s + L_a + G_r - 10 \log(T_s) - 10 \log(R) + 228.6 \quad (1)$$

The required inputs to formalize the link budget so as to calculate the E_b/N_0 are the peak transmitting power (P) in dBW, Line losses (L) in dB, Antenna Noise Temperature (Ta) in Kelvin, Frequency in Hz, Path length (R) in m, wavelength of the transmitted signal, diameter of the reflecting antenna, antenna efficiency, Transmit Antenna Gain (Gt) in dB, System Noise Temperature (Ts) in Kelvin and other miscellaneous losses like polarization loss, atmospheric losses, system losses and so on.

Table 1: Link Budget for ICM.

| Input Parameter | Symbol | Units | Value |
|-------------------------------------|-----------|-------|-----------|
| Frequency | f | GHz | 2.1 |
| Transmitter Power | P | dBW | 0 |
| Transmitter Line Loss | Lt | dB | -1 |
| Peak Transmit Antenna Gain | Gpt | dB | 8.25 |
| Transmit Antenna Diameter | Dt | m | 0.1 |
| Transmit Antenna Pointing Loss | Lpt | dB | -1 |
| Transmit Antenna Gain (Net) | Gt | dB | 7.25 |
| Equivalent Isotropic Radiated Power | EIRP | dBW | 6.25 |
| Propagation Path Loss (Max) | S | Km | 100 |
| Space Loss | Ls | dB | -158.89 |
| Polarization Loss | La | dB | -0.3 |
| Atmospheric Loss | Laa | dB | -1 |
| Receive Antenna Diameter | Dr | m | 0.5 |
| Peak Receive Antenna Gain | Grp | dB | 19.616 |
| Receive Antenna Pointing Loss | Lpr | dB | -1 |
| Received Isotropic Power | RIP | dBW | -147.56 |
| Receive Antenna Gain | Gr | dB | 15.946 |
| System Noise Temperature | Ts | dBK | 19.805 |
| Data Rate | R | kBps | 100 |
| E_b/N_0 | E_b/N_0 | dB | 26.638 |
| Carrier-to-Noise Density Ratio | C/No | dBHz | 79.308 |
| Bit Error Rate | BER | - | 10^{-6} |
| Required E_b/N_0 | E_b/N_0 | dB | 9.2 |
| Implementation Loss | - | dB | -10 |
| Margin | - | dB | 20.108 |

The antenna frequency is taken to be 2.1 GHz to reduce the antenna size and overcome interferences and attenuation. The transmitter power is taken as 1 W since only 100 kbps of raw data needs to be relayed. The transmitter line loss is taken to be -1 dB, estimated from the general lunar missions [8]. The peak transmit antenna gain is computed from the MATLAB simulations for the helical antenna. The transmit antenna diameter is chosen as 0.1 m to provide minimal sizing options. The transmit antenna pointing loss is estimated to be -1dB from the general lunar mission profiles [9]. The propagation path loss is 100 km considering a 100 km lunar frozen orbit. Transmit antenna gain Gt, space loss Ls and the EIRP are calculated from the equations.

$$G_t = G_{pt} + L_{pt} \quad (2)$$

$$EIRP = P + L_t + G_t \quad (3)$$

$$L_s = 147.55 - 20 \log S - 20 \log f \quad (4)$$

The polarization loss is estimated to be -0.3 dB using circular polarization. Since the Lune has no atmosphere, the atmospheric loss Laa is taken to be -1 dB accounting for random losses. The receiver antenna diameter is taken to be 0.5 m to again reduce the size. The peak receive antenna gain and the receive antenna pointing losses are taken to be 19.616 dB and -1 dB respectively, estimated from the lunar mission profiles [9].

The received isotropic power RIP and the receiver antenna gain Gr are calculated from the equations

$$RIP = E_b/N_0 - G_r/T_s - 228.60 + 10 \log R \quad (5)$$

$$G_r = G_{rp} + L_{rp} \quad (6)$$

The system noise temperature is estimated to be 19.805 dB-K [5]. The BER offset 10^{-6} achieved using QAM and Reed Solomon Turbo Channel Coding [5]. The required E_b/N_0 is 9.2 dB depending on the coding scheme, for example 9.2 for BPSK and 4.0 for 8FSK plus R-1/2 Viterbi Coding [5]. The implementation loss of -10 dB is estimated considering the miscellaneous space losses.

E_b/N_0 is calculated from the equation 1 and is found to be 26.638 dB. The carrier to noise density ratio C/No is calculated from the equation

$$C/N_0 = E_b/N_0 + 10 \log R \quad (7)$$

$$\text{Margin} = E_b/N_0 - \text{Req} E_b/N_0 \quad (8)$$

The link budget for a 100 km lunar orbit, transmitting at 100 Kbps to achieve BER of 10^{-6} for a transmission power of 1W and antenna gains of 8.25 dB using a helical antenna was calculated.

3. Results and Discussions

3.1. Link Budget

From the above observations, an E_b/N_0 of 26.638 dB with a margin of 20.108 dB for a BPSK modulated signal (which requires a minimum E_b/N_0 of 9.2) with hard convolution channel coding. This inference is supported by the MATLAB plots used for BER analysis for different modulation and channel coding techniques and show that efficient channel can be established using the set parameters. The channel coding is selected in reference to the MATLAB plots for BER analysis shows Hard Convolution suits the requirements and relatively easy to implement

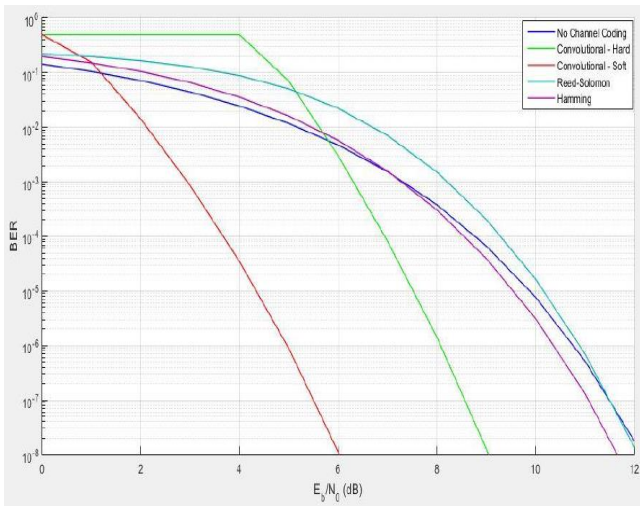


Fig. 5: BER v/s Eb/No plot for different channel coding.

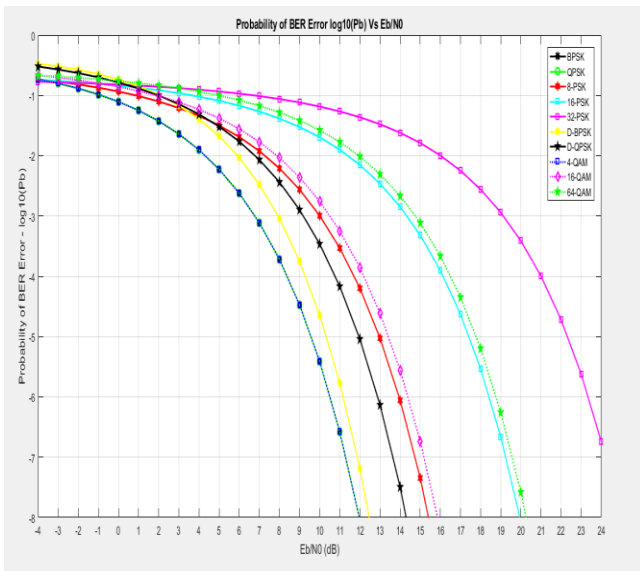


Fig. 6: BER v/s Eb/No plots for different modulation schemes

3.2. Antenna Modelling

The antenna most suitable for our research is modelled and simulated using MATLAB. The antenna designed was chosen so as to properly fit within the size constraints of Lunar Penetrator. A directional Helical Antenna was chosen with 8 turns. The parameters of the antenna are given as follows.

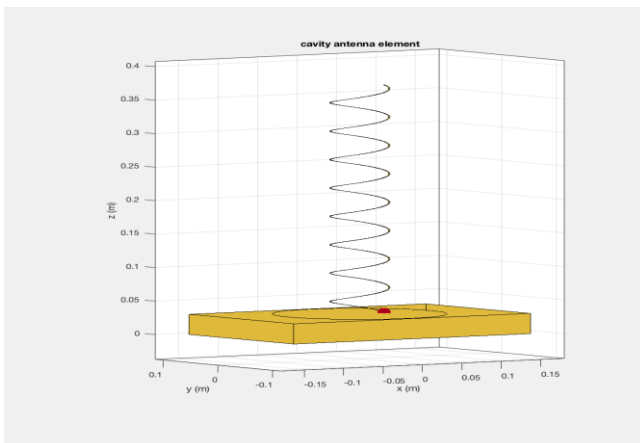


Fig. 7: Helical Antenna on the ICM with 8 turns with a center feed-point (using MATLAB).

Table 2: Antenna Parameters for the ICM.

| Parameter | Value |
|----------------------------|-------|
| Length (in m) | 0.30 |
| Width (in m) | 0.19 |
| Height (in m) | 0.03 |
| Spacing (in m) | 0.03 |
| Radius (in m) | 0.03 |
| Width (in m) | 0.001 |
| Turns | 8 |
| Spacing (in m) | 0.04 |
| Winding Direction | CCW |
| Substrate-cavity | Air |
| EpsilonR | 1 |
| Thickness (in m) | 0.03 |
| Ground Plane Radius (in m) | 0.09 |

The radiation patterns and the directivity in a 3D plane are analyzed and seen to suit our requirements of satellite communication.

The analysis and simulations yield an antenna suited for the ICM at 2.1 GHz show that such an antenna is realizable to support small lunar outreach programs. The resulting antenna adheres to the link budget and is the best choice for our module.

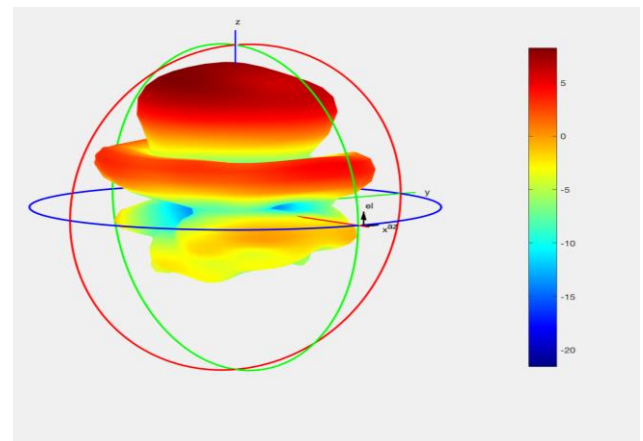


Fig. 8: 3D simulation of Antenna Radiation Pattern (using MATLAB).

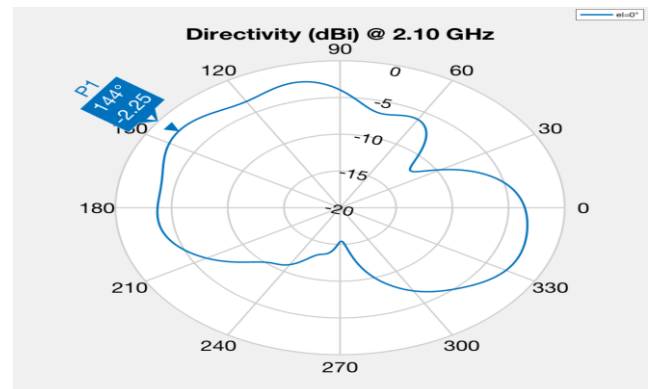


Fig. 9: A-Z pattern with maximum directivity of 144deg at 2.1GHz (using MATLAB).

3.3. Visibility Analysis

The in-orbit satellite, considering all favorable conditions communicates with the ICM aboard the Lunar Penetrator to establish a link in order to relay the raw observables. STK analysis shows a visibility time of approximately 15 minutes every 2.5 hours for a 100 km lunar orbit. Simulations were run, and real-time BER performance were recorded.

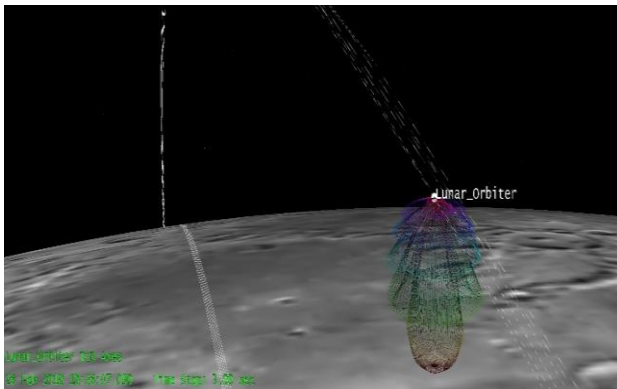


Fig. 10: 3D simulation of Antenna Radiation Pattern on-board the satellite (using STK).

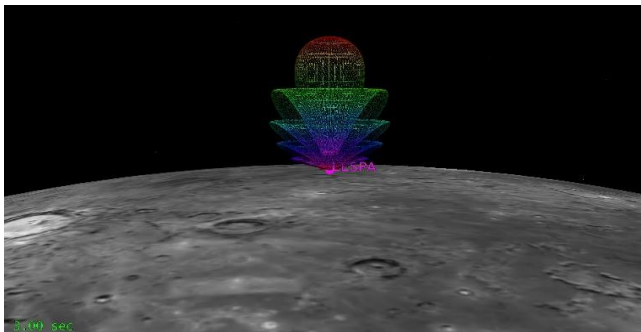


Fig. 11: 3D simulation of Antenna radiation patterns of ICM (using STK).

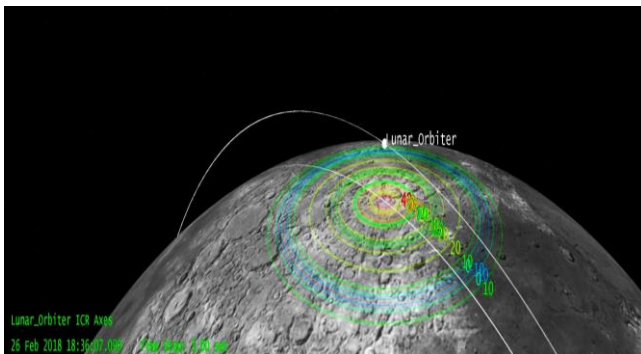


Fig. 12: 3D simulation of Antenna gain patterns of the satellite (using STK).

4. Conclusion

Analysis of the link budget was carried out for the ICM and favorable results were obtained at E_b/N_0 of 31.9 dB. BPSK modulation was chosen to support communication, with hard convolution channel coding. Further, a helical antenna was mounted as part of the ICM with a maximum directivity of 8.25 dB. The visibility for a 100km lunar orbit gives a view time of 15 minutes every 2.5 hours with one per million probabilities of error.

The ICM is designed with the aim to assist future small payload lunar missions and to improve student outreach in lunar exploration. The housing used for the ICM and the mini payload, i.e., the Lunar penetrator can be used for future payloads. This process ensures a modular approach which makes integration and management simple. Also, a model for link analysis will help all satellite mission, be it earth bound or interplanetary projects.

Acknowledgment

The authors would like to thank the final year project review panel at Department of ECE at SRM Institute of Science and Technolo-

gy for their valuable suggestions, and our seniors Mr. Sri Harsha Paluvuri and Mr. Akash Ratheesh for their help with device fabrication of LESPA.

References

- [1] Barad, K. R., Mody, A. A., Namdeo, S., Ratheesh, A., & Naik, K. P. (2017). SRMSAT-2: Study of the Lunar Sub-Surface and Deep-Space Environment Using a Micro-Satellite Platform. In 55th AIAA Aerospace Sciences Meeting (p. 0160).
- [2] Spencer, David B., Robert G. Melton, and Silvio G. Chianese. "Selecting Projects for a Capstone Spacecraft Design Course from Real World Solicitations." *Journal of Aviation/Aerospace Education & Research* 16.1 (2006).
- [3] Bame, S. J., Asbridge, J. R., Felthaus, H. E., Hones, E. W., & Strong, I. B. (1967). Characteristics of the plasma sheet in the earth's magnetotail. *Journal of Geophysical Research*, 72(1), 113-129
- [4] Earth's Magnetosphere and Plasmasphere available at https://www.nasa.gov/mission_pages/sunearth/multimedia/magnetosphere2-unlabeled.html#.WriRB4hubIU
- [5] Wiley J. Larson., *Space Mission Analysis and Design (SMAD)*, 1991.
- [6] Futaana, Y., Barabash, S., Wieser, M., Lue, C., Wurz, P., Vorburger, A., Bhardwaj, A. and Asamura, K., 2013. Remote energetic neutral atom imaging of electric potential over a lunar magnetic anomaly. *Geophysical Research Letters*, 40(2), pp.262-266.
- [7] Halekas, J.S., Delory, G.T., Lin, R.P., Stubbs, T.J. and Farrell, W.M., 2008. Lunar Prospector observations of the electrostatic potential of the lunar surface and its response to incident currents. *Journal of Geophysical Research: Space Physics*, 113(A9).
- [8] .Horányi, M., Sternovsky, Z., Lankton, M., Dumont, C., Gagnard, S., Gathright, D., Grün, E., Hansen, D., James, D., Kempf, S. and Lamprecht, B., 2014. The lunar dust experiment (LDEX) onboard the lunar atmosphere and dust environment explorer (LADEE) mission. *Space Science Reviews*, 185(1-4), pp.93-113.
- [9] Elphic, R.C. and Russell, C.T. eds., 2015. *The Lunar Atmosphere and Dust Environment Explorer Mission (LADEE)*. Springer.
- [10] Fahleson, U., 1967. Theory of electric field measurements conducted in the magnetosphere with electric probes. *Space Science Reviews*, 7(2-3), pp.238-262.